

Inducing Heat Reversal in a Three-Qubit Spin Chain

Saleh Naghdi,^{1,*} Thomas Quella,^{2,†} and Charles D. Hill^{1,2,‡}

¹*School of Physics, The University of Melbourne, Parkville, Victoria 3010, Australia*

²*School of Mathematics and Statistics, The University of Melbourne, Parkville, Victoria 3010, Australia*

(Dated: January 5, 2022)

By the standard second law of thermodynamics, heat spontaneously flows from a hotter body to a colder body. However, small-scale quantum systems in which quantum correlations play a prominent role can exhibit a non-classical reversal of such heat flow. We propose a quantum system consisting of an arbitrarily long chain of qubits existing in local Gibbs states, along which only adjacent qubits are allowed to thermally interact. By controlling quantum correlations along the chain, we then demonstrate non-classical heat reversal for the special case of a three-qubit chain on a quantum computer. We explore multiple initial conditions for the spin chain to showcase exotic behaviour such as the preferential pumping of heat afforded by unequal initial correlations between adjacent pairs of qubits, reinforcing the role that initial correlations play in influencing the dynamics of heat flow.

I. INTRODUCTION

Recent strides in quantum thermodynamics and quantum information science have discussed the role and utility of entanglement in giving rise to exotic thermodynamic behaviours [1] as it relates to entropy production [2], and anomalous equilibration [3]. This has consequently led to a variety of applications for quantum thermal machines and quantum heat engines [4] by using quantum coherence to control heat [5] and other thermodynamic properties [6] on a microscopic scale.

One result obtained from the work done by Partovi [7] challenges the classical notion that heat spontaneously flows from hotter to colder bodies - famously referred to as the thermodynamic arrow of time [8]. By proposing a particular entangled state between two multipartite quantum systems, Partovi shows that the anomalous reversal of heat flow from colder to hotter bodies can occur between systems that are initially quantum correlated. While peculiar in nature, this reversal effect emerges as a direct consequence of the quantum generalisation of the second law of thermodynamics which insists the change in the joint entropy of two systems is always non-negative.

This idea was investigated more concretely by Jennings and Rudolph [9] who examined the case of a three-qubit chain by way of simulations, using the initial condition in which the endmost qubits are correlated to showcase heat flow against the temperature gradient. Their work emphasises the complexity that initial correlations introduce to the flow of heat in a closed system. While Partovi, Jennings and Rudolph focused on a theoretical understanding of this phenomenon, it was not until recently that the reversal effect was experimentally observed by Micadei et al. for the simplest case of a pair of quantum correlated (as distinct from entangled) qubits prepared

in a solution, using Nuclear Magnetic Resonance (NMR) spectroscopy [10]. It is desirable to understand how more complex patterns of non-classical heat flow may arise by extending this setup to larger systems with more constituents.

In recent years, as noisy intermediate-scale quantum computers have emerged as a powerful device for simulating small-scale experiments, the field of quantum chemistry has enjoyed numerous advances in different areas, such as calculating the dipole moment of LiH in lithium-ion batteries [11], or learning the Hamiltonian of a quantum many-body system which has applications for statistical machine learning [12]. In this paper we harness the power of the IBM quantum computers to demonstrate the occurrence of heat reversal for the case of a quantum correlated three-qubit spin chain. We investigate in detail the complexity that switching on quantum correlations introduces to the heat flow by considering four individual initial conditions of interest outlined in Table I and henceforth referred to as “classical”, “reversal”, “preferential pumping”, and “local effects”. Our system is similar to the one analysed in Ref. 9 although, like Micadei et al., we additionally impose the condition that the qubits remain in a Gibbs state with respect to a fixed local Hamiltonian at all times. We describe an approach that is valid for a chain of N qubits, subsequently focusing on the special case of $N = 3$ for which we design a quantum circuit implementation that we run on the IBM quantum computers.

In what follows, we briefly touch upon the theoretical basis of the heat reversal phenomenon in quantum thermodynamics, and then outline the theoretical setup of our N -qubit chain, followed by the respective circuit implementation for $N = 3$ and the results associated with each of the four initial conditions.

A. Quantum Thermodynamics Background

When adapted to a quantum state described by the density matrix ρ , the quantum analogue of the second

* mnaghdi@student.unimelb.edu.au

† thomas.quella@unimelb.edu.au

‡ cdhill@unimelb.edu.au

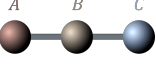
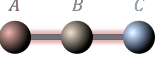
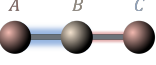
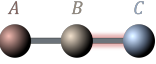
Case	Temperatures	Correlations
	$T_A > T_B > T_C$	$\alpha_{AB} = \alpha_{BC} = 0$
	$T_A > T_B > T_C$	$\alpha_{AB} < 0, \alpha_{BC} < 0$
	$T_A = T_C$	$-1 < \frac{\alpha_{BC}}{\alpha_{AB}} < 0$
	$T_A > T_B > T_C$	$\alpha_{BC} < \alpha_{AB} = 0$

TABLE I: Four initial conditions of interest for the three-qubit chain as described by three initial temperatures and two initial pairwise correlations. In descending order of rows, the cases follow: Classical, Reversal, Preferential Pumping, and Local Effects

law of thermodynamics reads

$$S(\rho_f || \rho_i) \geq 0, \quad (1)$$

where $S(\rho_f || \rho_i) = -\text{Tr}[\rho_f \log(\rho_i)] - S(\rho_f)$ is the quantum relative entropy of the final state ρ_f with respect to the initial state ρ_i , and $S(\rho) = -\text{Tr}[\rho \ln(\rho)]$ is the von Neumann entropy.

Consider two systems $i = (A, B)$ that are each initially in a Gibbs state of the local Hamiltonian \mathcal{H}_i :

$$\rho^i = \frac{e^{-\beta_i \mathcal{H}_i}}{\text{Tr}[e^{-\beta_i \mathcal{H}_i}]}, \quad (2)$$

where $\beta = \frac{1}{k_B T}$ and T is the temperature of the system. Provided that the evolution of the joint system $\rho^{AB} = \rho^A \otimes \rho^B$ is unitary and there is no work done throughout the evolution, it can be shown from (1) and the properties of the quantum relative entropy that [7, 10]

$$\beta_B Q_B + \beta_A Q_A = Q_B(\beta_B - \beta_A) \geq \Delta I(A : B). \quad (3)$$

Here, $I(A : B) = S(\rho^A) + S(\rho^B) - S(\rho^{AB}) \geq 0$ is the mutual information which is a measure of the degree of correlation between the two systems. Note that the right-hand side of (3) involves the *change* in mutual information, which may be negative.

Now let A be hotter than B ($\beta_A < \beta_B$). If A and B are initially uncorrelated, $\Delta I(A : B) \geq 0$. Thus

$$Q_B(\beta_B - \beta_A) \geq 0. \quad (3a)$$

It follows that $Q_B \geq 0$ and heat flows from A to B , as reminiscent of classical theory. In the presence of initial correlations, however, the mutual information can decrease $\Delta I(A : B) \leq 0$ so that the lower bound in (3) is relaxed. It is now possible that

$$Q_B(\beta_B - \beta_A) \leq 0, \quad (3b)$$

and heat can flow from cold to hot, $Q_B \leq 0$.

B. Theoretical Setup

We now consider the system of a linear chain of N spins in state ρ along which only adjacent pairs are allowed to thermally interact. We additionally subject the system to an external magnetic field in the \hat{z} direction so that the local Hamiltonian defining the initial state of each qubit as per Eq. (2) is

$$\mathcal{H}^i = \frac{1}{2} h \nu_0 (1 - \sigma_z^i), \quad (4)$$

where ν_0 is the Larmor frequency [10].

We wish to treat the individual qubits along the chain as thermodynamic systems of their own, as such the state variables of each qubit such as the temperature, and internal energy

$$U^i = \text{Tr}_i[\rho \mathcal{H}^i], \quad (5)$$

must be well-defined. This introduces a constraint on our system whereby the local state of each qubit $\text{Tr}_i[\rho]$ must remain a Gibbs state (refer to (2)) with respect to (4) throughout the course of its evolution. We will call this constraint the Local Gibbs Criterion (LGC), which will be accounted for in the following characterisation of the initial state and evolution of our system.

1. Initial State

We use the definition of the initial state introduced by Meicadei et al. [10] for a chain of two qubits i and j ,

$$\rho_0^{i,j} = \rho_0^i \otimes \rho_0^j + \chi^{i,j}, \quad (6)$$

to define the initial state

$$\rho_0 = \sum_{i=1}^{N-1} \rho_0^{1 \rightarrow i-1} \otimes \rho_0^{i,i+1} \otimes \rho_0^{i+2 \rightarrow N} - (N-2) \rho_0^{1 \rightarrow N}, \quad (7)$$

for a chain of $N \geq 3$ qubits, where the second term in (7) is incorporated to offset the double-counting of diagonal terms in the resultant mixed state, and $\rho_0^{i \rightarrow j} = \bigotimes_{k=i}^j \rho_0^k$ is adopted as shorthand notation.

Crucially, this definition of the spin chain allows to incorporate correlations for every adjacent pair of qubits. This is achieved by the inclusion of the $\chi^{i,j}$ term in Eq. (6) which in this paper is chosen to be

$$\chi^{i,j} = \begin{bmatrix} 0 & 0 & 0 & 0 \\ 0 & 0 & \bar{\alpha}_{i,j} & 0 \\ 0 & \alpha_{i,j} & 0 & 0 \\ 0 & 0 & 0 & 0 \end{bmatrix} \quad (8)$$

and captures the initial correlations between qubits i and j [10]. The parameter $\alpha_{i,j}$ is a measure for the correlations between the two qubits and its value is chosen to preserve the positivity of ρ_0 . Since $\text{Tr}_i[\chi_{AB}] = 0$, it is

ensured that introducing correlations of this form does not alter the condition that the qubits remain in a local Gibbs state with respect to the Hamiltonian (4) and so have a well-defined internal energy (5) and temperature. Moreover, the reduced density matrix obtained by tracing out all but a given adjacent pair of qubits resembles the form of (6) so that the correlation terms can be read off.

In total, there are $2N-1$ parameters defining the initial state of the chain: N temperatures $\mathbf{T} = (T_1, \dots, T_N)$ and $N-1$ nearest-neighbour correlations $\boldsymbol{\alpha} = (\alpha_1, \dots, \alpha_N)$.

2. Thermalisation operator

We recall from Refs. [9, 10] that the thermalisation of two qubits is described by a Dzyaloshinskii–Moriya (DM) interaction

$$\mathcal{H}_{DM}^{i,j} = (\hbar/2)J(\sigma_x^i \sigma_y^j - \sigma_y^i \sigma_x^j), \quad (9a)$$

where the frequency J is a parameter. For the N -qubit chain, we make the extension

$$\mathcal{H}_{DM} = \sum_{i=1}^{N-1} \mathcal{H}_{DM}^{i,i+1}, \quad (9b)$$

to allow for simultaneous thermalisation between all adjacent pairs, which yields the time evolution operator

$$U_\tau = e^{-i\tau \mathcal{H}_{DM}/\hbar}. \quad (10)$$

Importantly, since the thermalisation operator commutes with the sum of local Hamiltonians,

$$\left[\sum_{i=1}^N \mathcal{H}^i, \mathcal{H}_{DM} \right] = 0,$$

thermalisation does not perform work on the individual qubits. It can be shown that as a consequence of this, the local Hamiltonians remain unchanged throughout the evolution – in line with the LGC [7]. Moreover, due to no work being done, at a given time τ the change in mean energy of either system is due completely to the heat: $Q^i = \Delta U^i$. Thus, heat flow may be inferred by calculating the energy of each qubit according to Eq. (5) as a function of time. It should be noted that in general, evolving the initial state defined in Eq. (7) according to the evolution operator in Eq. (10) also introduces correlations between non-neighbouring qubits. Compared to the correlations between adjacent qubits these are relatively weak.

II. CIRCUIT IMPLEMENTATION FOR THE CASE OF THREE QUBITS

We now use a quantum computer to simulate the heat flow along the three-qubit chain where $N = 3$ and $i = (A, B, C)$. Table I shows four different instances of theoretical interest:

- **Classical:** The classical case contains a thermal gradient $A \rightarrow C$ but without initial correlations existing between any adjacent pair of qubits. As a result, we expect the initial heat flow to be in the direction of the temperature gradient as would be predicted by classical thermalisation.
- **Reversal:** The reversal case contains a similar temperature gradient to the classical case, except that now there exist nonzero initial correlations between both adjacent pairs of qubits, α_{AB} and α_{BC} . This is the generalised form of the original case of two correlated qubits demonstrated in Ref. 10.
- **Preferential pumping:** In this case, we explore the effect of the magnitude of initial correlations on heat flow. To achieve this, we set the temperatures of the two endmost qubits $T_A = T_C$ to be the same and hotter than the middle qubit, while enforcing stronger correlations between A and B , than B and C . Ignoring correlations – as one would in a classical regime – we expect the heat flow to be symmetric with the same amount of heat leaving both A and C to be absorbed by B .
- **Local effects:** This case follows almost the same set-up as the reversal case, except we remove correlations between one of the adjacent pairs, so that $\alpha_{AB} = 0$. Here we probe how a local heat reversal between B and C might influence the heat flow of A which initially is not correlated with the rest of the system and thus expected to be classical.

In line with the layout presented in Section IB, the schematic layout of our circuit implementation shown in Fig. 2a consists of two routines: initial state preparation (Fig. 2b), and evolution (Fig. 2c). Both these routines

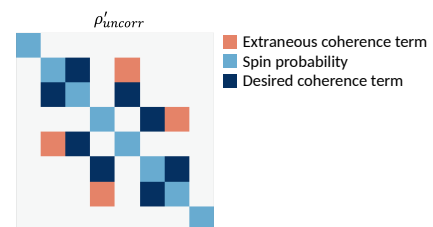


FIG. 1: An illustration of the general initial density matrix ρ'_{uncorr} produced by the ansatz shown in Figure 2b. Note that the structure almost completely resembles our definition in Eqn. (7), with the exception of the orange entries which are the extraneous correlations between A and C introduced by our construction. The diagonal terms in light blue correspond to the probability distribution of the chain's spin states, and entries in dark blue correspond to the desired correlations.

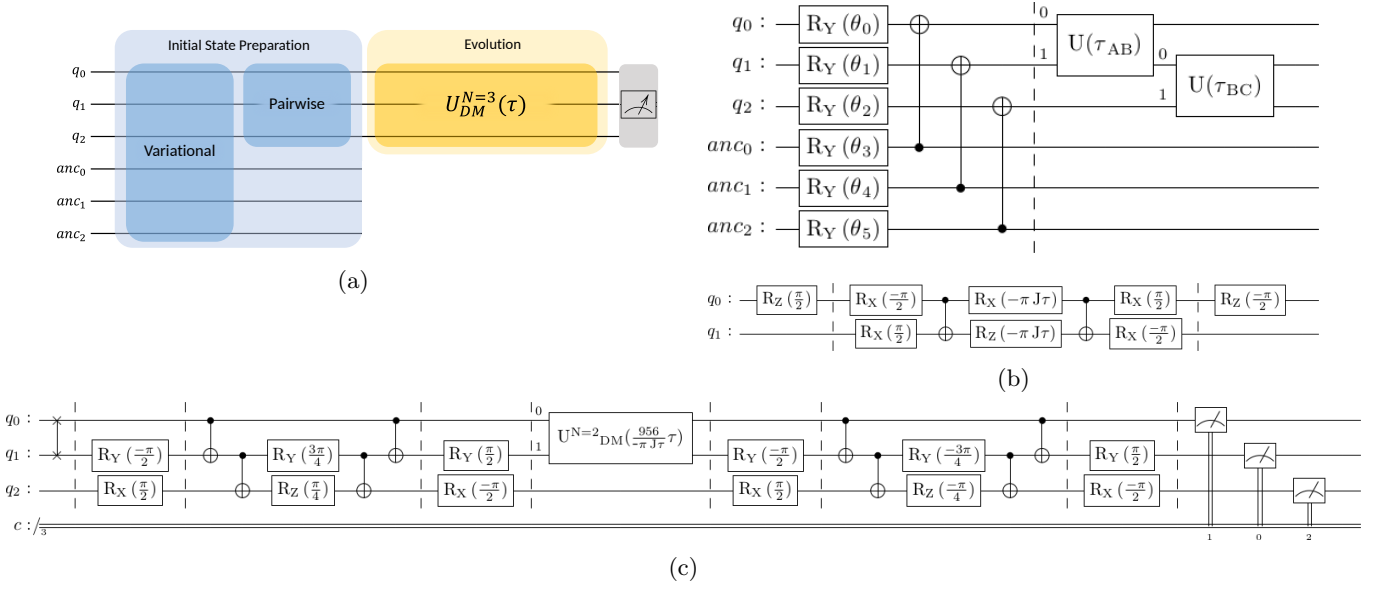


FIG. 2: The relevant components of the circuit implementation for the three-qubit spin chain. (a) outlines the schematic layout of the circuit which consists of two stages: initial state preparation (b) and evolution (c). The initial state preparation (b) itself involves a *variational* step for preparing an uncorrelated state (left of barrier), and a *pairwise* step for generating correlations (right of barrier). Note the label *anc* for the bottom three qubits denotes the ancillary register, while the top three are system qubits. Below this, the two-qubit thermalisation subroutine $U_{DM}^{N=2}$ generated by the Hamiltonian (9a). The evolution stage (c) includes the Cartan circuit decomposition for $U_{DM}^{N=3}$ which makes use of $U_{DM}^{N=2}$; Optimisations made to the conjugate terms come at the expense of an initial swap gate whose effect is reversed during measurement by redirecting qubit correspondence to the classical register.

will rely on a posteriori data obtained from classical simulations made possible by the sufficiently small size of the system.

A common subroutine that will be used in what follows is the pairwise evolution operator defined in Eqn. (10) for $N = 2$, the circuit implementation of which can be seen in Fig. 2b.

1. Initial State Preparation

We now hope to prepare the initial state given in Eq. (7). Our strategy is to create an uncorrelated chain first, onto which we then generate the desired correlations.

a. Uncorrelated state preparation An uncorrelated state corresponds to a diagonal density matrix in which all off-diagonal coherence terms are zero. For the definition introduced in Eq. (7), this corresponds to setting the correlation terms $\alpha = \mathbf{0}$. Such a state may be prepared using a variational circuit (Fig. 2b) which is parameterised by twelve Y-rotation angles θ and entangles every qubit in the chain with a respective ancilla qubit. As a result, the number of qubits in our register totals $2N = 6$ and the state ρ'_{uncorr} of the chain is recovered by tracing out the ancillary register.

We then use a classical optimiser (viz. Gradient descent) with a Manhattan distance loss function to obtain

the rotation angles that best approximate ρ'_{uncorr} to a provided ρ_{uncorr} .

b. Generating correlation terms The general form of Eq. (7) can be approximated by applying two consecutive two-qubit operators (Figure 2b) parametrised by propagation times τ_{AB} and τ_{BC} to each of the two pairs (A, B) and (B, C) respectively, obtaining ρ'_{corr} .

When this construction (Fig. 2b) is applied to a diagonal state for arbitrary propagation times, the resultant ρ'_{corr} has off-diagonal terms located in the same location as what would be produced had it been evolved using U_{τ}^3 . That is, this method of preparation generates two extraneous off-diagonal terms which correspond to correlation between the A and C , α_{AC} (Figure 1), effectively wrapping our chain into a ring. Nonetheless, the magnitude of the undesirable correlations remains negligible compared to α_{AB} and α_{BC} .

The goal now becomes tuning $\tau = (\tau_{AB}, \tau_{BC})$ to obtain the cases of interest in Table I. We obtain $\alpha(\tau)$ and $\mathbf{T}(\tau)$ from ρ'_{corr} . Note that $\alpha(\mathbf{0}) = \mathbf{0}$ yields the classical case so long as the uncorrelated state prepared had been one in which $\mathbf{T}(\mathbf{0}) = (T_A, T_B, T_C)$ satisfied $T_A > T_B > T_C$. Depending on the case under discussion, we may now choose a relevant cost function with arguments $\alpha(\tau)$ and $\mathbf{T}(\tau)$ that when optimised using a classical optimiser returns a solution that satisfies the conditions of the case.

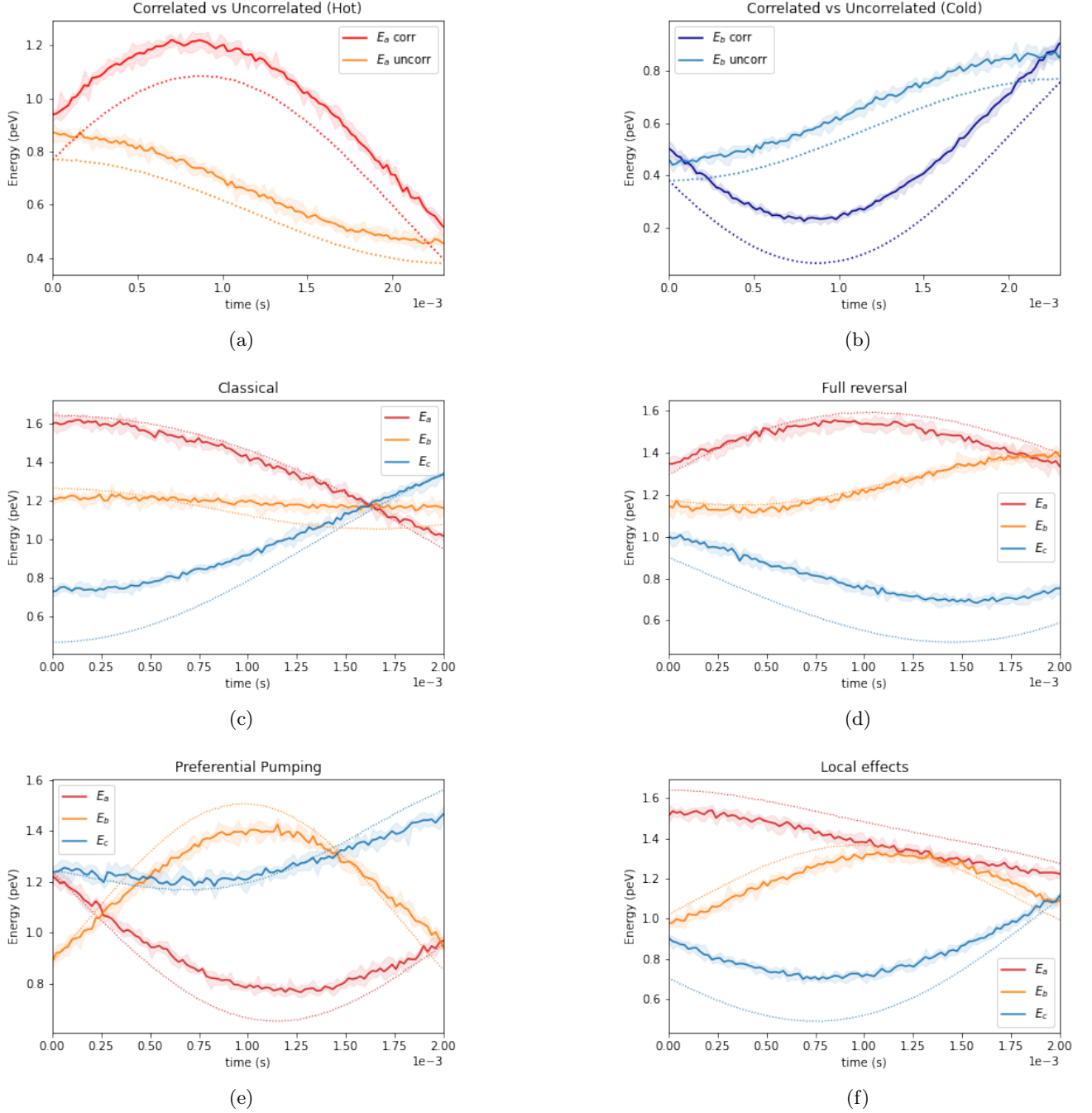


FIG. 3: The reproduced heat flow for the two-qubit case [10] consisting of a hot (a) and cold (b) qubit. (c)-(f) display the heat flow for the three-qubit case under the different instances mentioned in Table I including classical (c), reversal (d), preferential pumping (e), and local effects (f). Results were obtained by running on the Qiskit *ibmq_toronto* backend, averaged over 6 trials each consisting of 8192 shots. Shown in dotted are the simulation predictions.

2. Thermalisation operator

One obvious circuit implementation for U_τ^3 is a Suzuki–Trotter approximation which would involve repeated application of the second half of the circuit shown

in Figure 2b. However, depending on the margin of error required, this method can quickly become costly in terms of circuit depth and particularly the number of CNOT gates. Alternatively, we may obtain a relatively inexpensive and fixed-depth implementation by obtaining a

Cartan decomposition [13] which requires 18 CNOTs and makes use of U_τ^3 . A further reduction to 13 CNOTs can be made by condensing the conjugate terms involved in the decomposition to yield the circuit in Fig. 2c.

Our key goal in the design of the circuits is minimising the circuit depth so as to reduce the noise in the energy readings. In particular, we wish to minimise the CNOT count and avoid the use of SWAP gates by applying CNOTs only between qubits that are neighbouring with respect to the coupling map of the IBM quantum machine being used.

III. RESULTS AND DISCUSSION

Fig. 3 displays the heat flows for both the reproduced two-qubit case [10], as well as the four instances of the extended three-qubit case. The results were obtained by running on the 27-qubit IBM quantum backend *ibmq_toronto*, where measurement error mitigation was used to reduce readout errors. The coupling map of this backend provided several choices for an optimal group of six physical qubits on which to run the circuit implementation for the three-qubit chain [14]. Ultimately, the subset of qubits chosen was that which yielded initial energy measurements at $\tau = 0$ which were closest to the theoretical values. It was assumed that the subset which met this criterion would also offer results that were closest to the overall theoretical heat flow curve for all other times. In measuring the quantumness of the initial correlations the Geometric Quantum Discord (GQD) ADD REF was calculated for each pair of qubits (using the initial density matrix as obtained by state tomography) and then compared to the theoretical values.

Figs. 3a and 3b display the reproduced results for heat flow between two qubits as originally investigated in depth by Micadei et al. using an NMR setup [10]. The energy of the hotter qubit shown in Fig. 3a initially increases (decreases) in the correlated (uncorrelated) case, showcasing heat reversal as brought upon by introducing quantum correlations. The opposite effect occurs for the energy of the colder qubit shown in Fig. 3b.

By analogy, Figs. 3c and 3d show the difference in heat flow between the classical and correlated cases respectively for our extended three-qubit system. The GQDs between the pairs A & B, and B & C, in the initial state of the correlated case are 0.023 and 0.017 respectively, dominating the corresponding values of 1×10^{-3} and 8×10^{-3} obtained in the uncorrelated case. As a result, while in Fig. 3c heat is shown to flow classically along the temperature gradient $A \rightarrow B \rightarrow C$, introducing correlations α_{AB} and α_{BC} induces a full reversal of the heat flow in the direction $C \rightarrow B \rightarrow A$ as seen in Fig. 3d. The times at which the hottest and coldest qubits each obtain their energy extrema appear to be out of phase, unlike in the two-qubit case, which highlights the role of the intermediate qubit both as a conduit as well as a storage of heat.

It should be noted that while, theoretically, it would

be expected for the GQD between any pair of qubits to evaluate to zero in the uncorrelated case, the fact that it is still nonzero indicates the presence of noise introducing some amount of quantum correlations. Indeed, even running an empty circuit produces a state that is similarly quantum correlated – if only weakly so – which implies that even the initial state is not necessarily $|\bar{0}\rangle$. It must also be mentioned that the density matrix used in the GQD calculations was obtained by state tomography whose circuit implementation is equally prone to noise.

In Fig. 3e, we observe more clearly the role of quantum correlations as a heat pump. By having $|\alpha_{AB}| > |\alpha_{BC}|$, the GQD between A and B (0.023) evaluates to be almost an order of magnitude larger than the GQD between B and C (4×10^{-3}). As a result, despite there being a symmetric temperature distribution, qubit A is the preferred heat source for the central qubit B, even though both A and C are initially at the same temperature.

Finally, by tweaking the full reversal case to allow relatively large correlations between only one adjacent pair, we can restrict heat reversal only to that pair alone. This is seen in Fig. 3e for the pair B and C (GQD: 0.015) compared to the pair A and B (GQD: 4×10^{-3}), as qubit A continues to thermalise classically, albeit at a slower rate due to the anomalous heating of its neighbour B which is correlated with C. This reveals a property of locality in the proposed generalisation, in that the heat reversal appears to only occur between neighbours that share a correlation.

The slight inconsistency in the results for the three-qubit case against the simulated predictions may be explained by the presence of errors in as early as the variational step which despite being intended for preparing an uncorrelated and diagonal state still exhibits off-diagonal terms as shown in the heatmap of Fig. 4a, implying that the starting state is not always the $|0\rangle$ state. In Fig. 4b we see that these errors are dispersed throughout the mixture during the pairwise stage of initial state preparation, and then intensified after the evolution stage Fig. 4c, which for the case of $\tau = 0$ has the benign effect of only increasing the circuit depth, and thus, the chance for errors to propagate. This is further emphasised by the close correspondence between numerically evolving the state obtained via state tomography and the real results in Fig. 4d which suggests that the evolution stage is not the main source of error. In addition to this, the systematic overestimation of the real trials compared to the predicted results for the two-qubit case in Figs. 3a and 3b suggests the presence of model bias, which is reminiscent of a thermal relaxation error caused by short thermal relaxation time T_1 .

IV. CONCLUSION

We have extended the demonstration of anomalous heat flow in quantum systems to spin chains, demon-

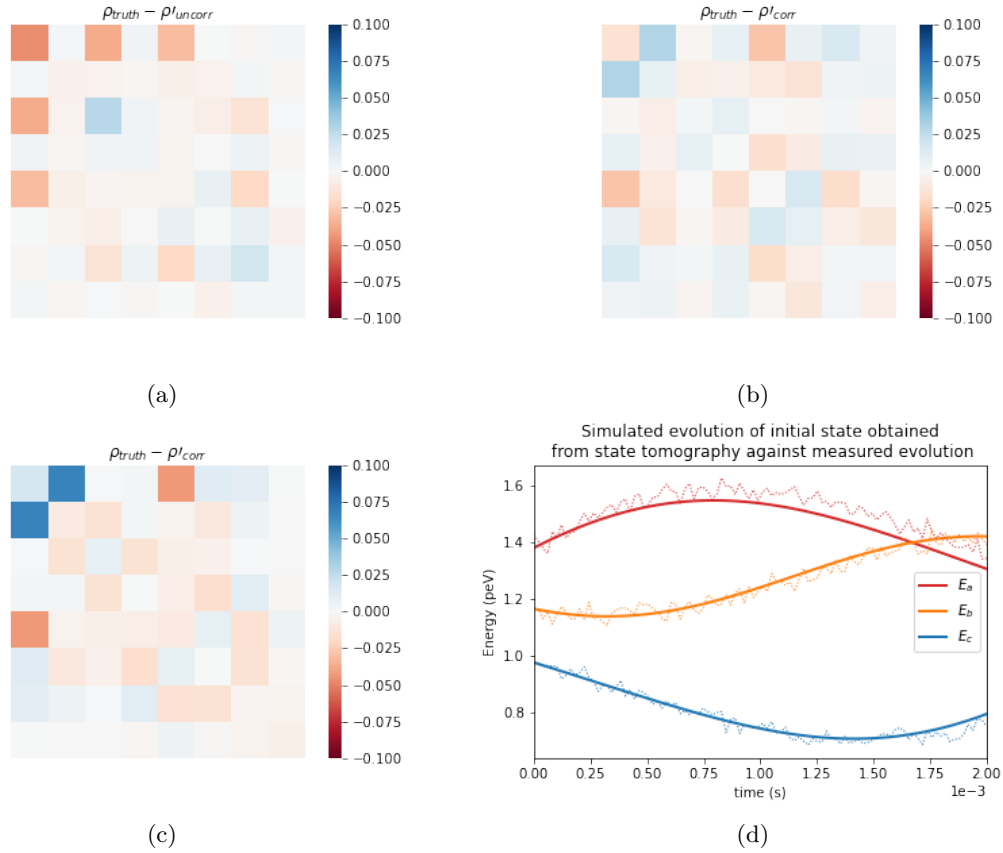


FIG. 4: The error in the measured state at $\tau = 0$ for the reversal case, obtained by state tomography, compared to the theoretical state at three different stages along the final circuit implementation: variational (a), pairwise (b), and evolution (c). The errors emerge as a result of unwanted qubit thermal relaxation and rotation. (d) shows the correspondence between the heat flow obtained by measurement, and that obtained by numerically evolving the measured initial state as reconstructed by state tomography.

strating it explicitly for three-qubit systems. This extends previous results obtained by Micadei et al. for the limiting case of a two-qubit chain [10].

By utilising the greater variety in initial conditions afforded by the jump to three qubits, we demonstrated four main examples. These include classical thermalisation, full and partial anomalous heat reversal, and the preferential pumping of heat in an initially symmetric temperature profile. The results provide further experimental verification of the nature of decreasing quantum correlations as an entropic process which can offset the entropy consumed during heat reversal. The results for cases like preferential pumping may also hint at the utility of correlations as a means of precisely controlling heat in small systems.

One may consider a circuit implementation for a spin chain of arbitrary length by following a similar procedure to the special case of the three-qubit chain. However, extending this to large lengths is currently limited by the a posteriori simulation data that is used to fix the parameters for initial state preparation. As far as uncorrelated state preparation is concerned, a priori meth-

ods have been devised for preparing Gibbs states [15], but even still the task of generating correlations remains nontrivial.

One point of interest for future work is experimental demonstration of anomalous heat flow in systems more complex than a linear chain of qubits where additional exotic effects may emerge, such as a system of qudits. A possible extension to the setup may involve making the system non-isolated by having it interact with an external thermal bath such as the one defined in Ref. 16. This would allow closer modelling of the dissipation of heat which is more physically accurate than assuming that the system is closed and no heat is lost. In this scenario, fine-tuning initial correlations may be utilised to achieve more ambitious thermodynamic goals, such as thermally insulating the system from the bath.

ACKNOWLEDGMENTS

This work was supported by the University of Melbourne through the establishment of an IBM Quantum Network Hub at the university. C.D.H. is supported through a Laby Foundation grant at the University of

Melbourne. T.Q.'s research was conducted at the Australian Research Council (ARC) Centre of Excellence for Mathematical and Statistical Frontiers (ACEMS, project number CE140100049) and partially funded by the Australian Government.

-
- [1] N. H. Y. Ng and M. P. Woods, Resource Theory of Quantum Thermodynamics: Thermal Operations and Second Laws, in *Thermodynamics in the Quantum Regime: Fundamental Aspects and New Directions*, Vol. 195, edited by F. Binder, L. A. Correa, C. Gogolin, J. Anders, and G. Adesso (2018) p. 625.
 - [2] G. T. Landi and M. Paternostro, Irreversible entropy production: From classical to quantum, *Reviews of Modern Physics* **93**, 035008 (2021).
 - [3] P. C. Lotshaw and M. E. Kellman, Asymmetric temperature equilibration with heat flow from cold to hot in a quantum thermodynamic system, *Phys. Rev. E* **104**, 054101 (2021), arXiv:2106.08508 [cond-mat.stat-mech].
 - [4] P. A. Camati, J. F. Santos, and R. M. Serra, Coherence effects in the performance of the quantum Otto heat engine, *Physical Review A* **99**, 062103 (2019).
 - [5] R. Biele, C. A. Rodríguez-Rosario, T. Frauenheim, and A. Rubio, Controlling heat and particle currents in nanodevices by quantum observation, *npj Quantum Materials* **2**, 1 (2017).
 - [6] J. F. Santos, C. H. Vieira, and P. R. Dieguez, Negativity-mutual information conversion and coherence in two-coupled harmonic oscillators, *Physica A: Statistical Mechanics and its Applications*, 125937 (2021).
 - [7] M. H. Partovi, Entanglement versus Stosszahlansatz: Disappearance of the thermodynamic arrow in a high-correlation environment, *Physical Review E* **77**, 021110 (2008).
 - [8] D. V. Schroeder, *An introduction to thermal physics* (Oxford University Press, 2021).
 - [9] D. Jennings and T. Rudolph, Entanglement and the thermodynamic arrow of time, *Physical Review E* **81**, 061130 (2010).
 - [10] K. Micadei, J. P. Peterson, A. M. Souza, R. S. Sarthour, I. S. Oliveira, G. T. Landi, T. B. Batalhão, R. M. Serra, and E. Lutz, Reversing the direction of heat flow using quantum correlations, *Nature communications* **10**, 1 (2019).
 - [11] J. E. Rice, T. P. Gujarati, M. Motta, T. Y. Takeshita, E. Lee, J. A. Latone, and J. M. Garcia, Quantum computation of dominant products in lithium-sulfur batteries, *The Journal of Chemical Physics* **154**, 134115 (2021).
 - [12] A. Anshu, S. Arunachalam, T. Kuwahara, and M. Soleimanifar, Sample-efficient learning of interacting quantum systems, *Nature Physics*, 1 (2021).
 - [13] E. Kökcü, T. Steckmann, J. Freericks, E. F. Dumitrescu, and A. F. Kemper, Fixed depth Hamiltonian simulation via Cartan decomposition, arXiv preprint arXiv:2104.00728 (2021).
 - [14] Optimal in the sense of not requiring any additional SWAP gates to accommodate CNOTs between any pair of qubits along the circuit.
 - [15] C. Zoufal, A. Lucchi, and S. Woerner, Variational quantum Boltzmann machines, *Quantum Machine Intelligence* **3**, 10.1007/s42484-020-00033-7 (2021).
 - [16] V. Scarani, M. Ziman, P. Štelmachovič, N. Gisin, and V. Bužek, Thermalizing quantum machines: Dissipation and entanglement, *Physical review letters* **88**, 097905 (2002).